10th ANKARA INTERNATIONAL AEROSPACE CONFERENCE **AIAC-2019-098**
18-20 September 2019 - METU, Ankara TURKEY

NUMERICAL CALCULATIONS OF MAGNUS FORCE AND MOMENT ON ROTATING MISSILES WITH DIFFERENT FIN CONFIGURATIONS

Batuhan Nasuhbeyoğlu[1], Kıvanç Arslan[2] and Emrah Gülay[3]
ROKETSAN Missile Industries Inc.
Ankara, Turkey

ABSTRACT

For missiles spinning at high rotational rates, it is important to consider Magnus force and moment to calculate the trajectory and aerodynamic performance of the projectile correctly. Significant Magnus effects are present especially on missiles at high angles of attack. In this paper, it is aimed to calculate Magnus dynamic derivatives and roll damping coefficient numerically for three different missile configurations. First, a validation study is performed to compare numerical results with experiment. Then, the effect of fin aspect ratio to Magnus characteristics of spinning missiles is examined. It is found that very low aspect ratio fins result in low Magnus force, Magnus moment and roll damping coefficients.

INTRODUCTION

When a projectile spins through the air at a finite angle of attack, a side force, known as Magnus force, and its moment counterpart, Magnus moment, is generated due to non-symmetrical pressure distribution on the right and left sides of the body. The reason for this unequal pressure distribution is viscous interaction between the fluid and projectile surface [Bhagwandin, 2016]. For finned missiles, it is known that not only the body but also fin geometry has a significant effect on Magnus force and moment [Pechier, 2001]. In addition to static and dynamic aerodynamic coefficients, calculation of Magnus force and moment for spinning missiles is necessary for the determination of trajectory and aerodynamic performance correctly. Significant amounts of Magnus force and moment are generated on a missile that has high spin/angular velocity at high angles of attack. Magnus force and moment can be calculated from flight tests, wind tunnel tests, CFD methods and empirical methods. Improvements in computing capacity make the employment of CFD methods for Magnus calculations more feasible ever than before.

Definitions of Magnus force, Magnus moment and roll damping moment used in this study are given in equations 1 to 3. Since the change of Magnus force and moment with the angle of attack is non-linear, each analysis is performed for a constant angle of attack. Therefore, C_{Y_P} and C_{n_P} coefficients are calculated instead of traditional $C_{Y_{p_\alpha}}$ and $C_{n_{p_\alpha}}$ coefficients.

[1] Senior Engineer, Aerodynamic Design and Analysis Department, Email: bnasuhbeyoglu@roketsan.com.tr
[2] Senior Engineer, Aerodynamic Design and Analysis Department, Email: kivanc.arslan@roketsan.com.tr
[3] Chief Engineer, Aerodynamic Design and Analysis Department, Email: egulay@roketsan.com.tr

Definitions of C_{Y_P}, C_{n_P}, C_{l_P} and non-dimensional spin rate (Ω) are given in equation 4 [Bhagwandin, 2016].

$$Magnus\ Force = \frac{1}{2}\rho V^2 S\left(\frac{pD}{2V}\right)C_{Y_p} \tag{1}$$

$$Magnus\ Moment = \frac{1}{2}\rho V^2 S\left(\frac{pD}{2V}\right)C_{n_p} \tag{2}$$

$$Roll\ Damping\ Moment = \frac{1}{2}\rho V^2 SD\left(\frac{pD}{2V}\right)C_{l_p} \tag{3}$$

$$C_{Y_p} = \frac{\partial C_Y}{\partial \Omega}rad^{-1}, \quad C_{n_p} = \frac{\partial C_n}{\partial \Omega}rad^{-1}, \quad C_{l_p} = \frac{\partial C_l}{\partial \Omega}rad^{-1}, \quad \Omega = \frac{pD}{2V}rad \tag{4}$$

In the first part of this paper, wind tunnel test results of "Modified Basic Finner (MBF)" [Jenke, 1976] test case model are used to verify numerical approach employed to calculate Magnus force and moment coefficients. In the second part of the paper, Magnus force, Magnus moment and roll damping coefficients of two additional missile configurations with different fin aspect ratios are calculated with verified CFD method. Effects of fin aspect ratio on Magnus force, Magnus moment and roll damping coefficients are examined.

METHOD

The geometry of MBF test case model, axis system used in calculations, computational domain and details of CFD methodology is explained in this section.

Geometry of the MBF Test Case Model

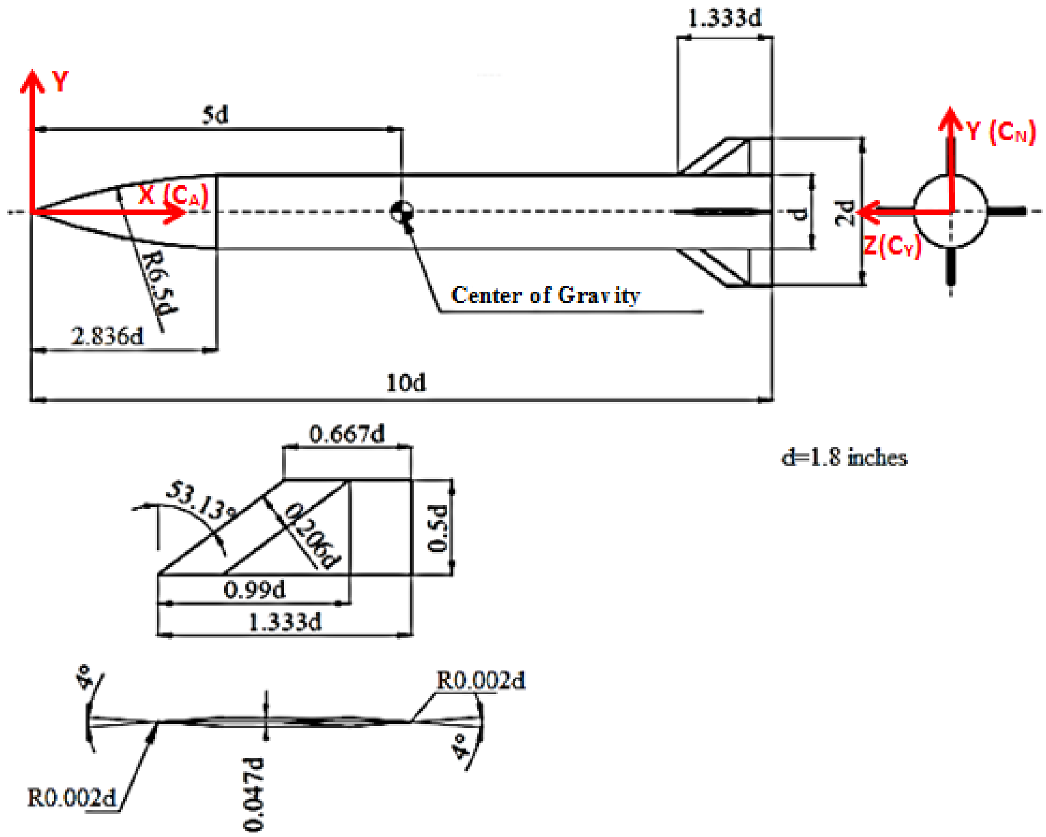

Figure 1: "Modified Basic Finner" Geometry Details [Bhagwandin, 2012; Jenke, 1976]

Geometric details of the MBF test case model and coordinate system used in analyses are given in Figure 1.

Computational Mesh and Numerical Method

Flowfield around the missile is modeled by using Navier-Stokes equations. In order to numerically model Navier-Stokes equations, an unstructured mesh is generated for the whole solution domain. Before starting analyses, a couple of meshes with different qualities are generated and CFD analyses are performed for grid convergence to use the most suitable mesh quality in the following analyses. Mesh of the model is generated by considering y+=1 and Mesh domain consists of about 8.5 million elements. GAMBIT and TGRID commercial software are used to generate the solid model and computational domain. Details of the computational domain can be seen from Figure 2.

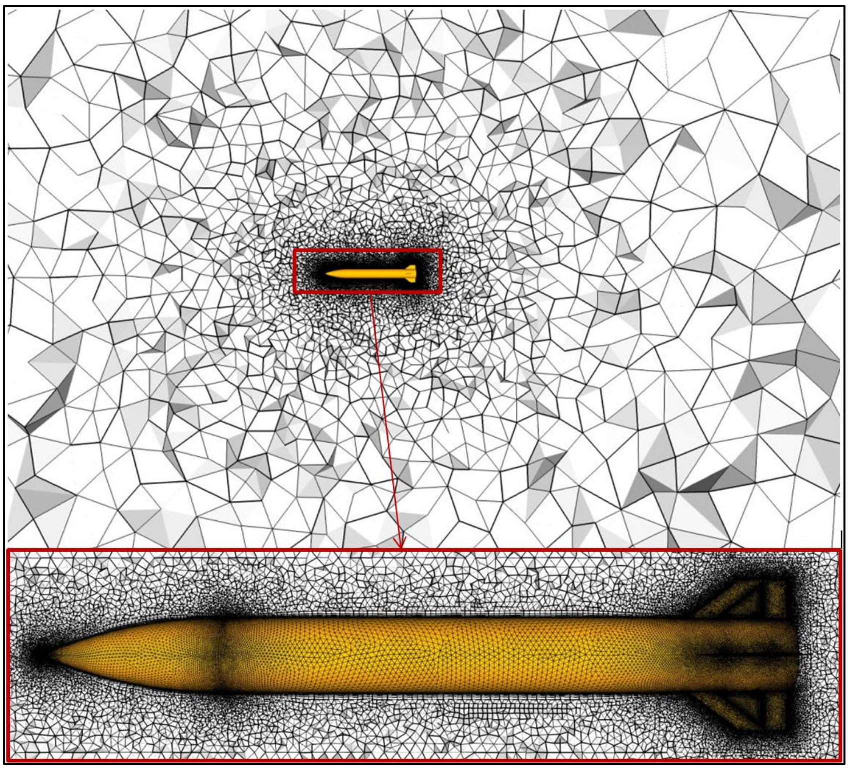

Figure 2: Mesh of the Model

In order to calculate Magnus force, Magnus moment and roll damping moment coefficients, transient aerodynamic analyses are done. Analyses are performed using CFD++ commercial computational fluid dynamics software.

Boundary Conditions and Flowfield Modelling

For verification study, results from “Arnold Engineering Development Center (AEDC)” wind tunnel at test conditions given in Table 1 [Jenke, 1976] are used. Accordingly, CFD analyses are done at the same conditions.

Table 1: Wind Tunnel Test Conditions

M	2.5
Re_d	$4.1x10^5$
P_0	98320 Pa
T_0	311.1 K

In order to start unsteady analyses, initial values are calculated using steady analyses. Then, the whole solution domain is rotated for unsteady analyses. Flowfield is modeled at 2.5 Mach for different angles of attack, using Realizable k-ε turbulence model.

CFD analyses are performed at 0.03 non-dimensional spin rate (Ω). For 2.5 Mach and 0.03 non-dimensional spin rate, angular velocity becomes 773.3 rad/s. The domain is rotated 3 times for convergence. Time step for analyses is set as $1x10^{-5}$ seconds and 50 inner iterations for each time step are carried out. The global coordinate system is used in the analyses, which is not rotating with body.

VERIFICATION RESULTS

Unsteady CFD analyses are done at 10º, 20º, 30º, 40º, 50º and 60º angle of attacks (in xy plane) with Mach number is equal to 2.5. In Figure 3-5, results obtained for side force coefficient, yaw moment coefficient and roll moment coefficient at 20º angle of attack for 0.03 seconds (3.6 revolutions) are shown.

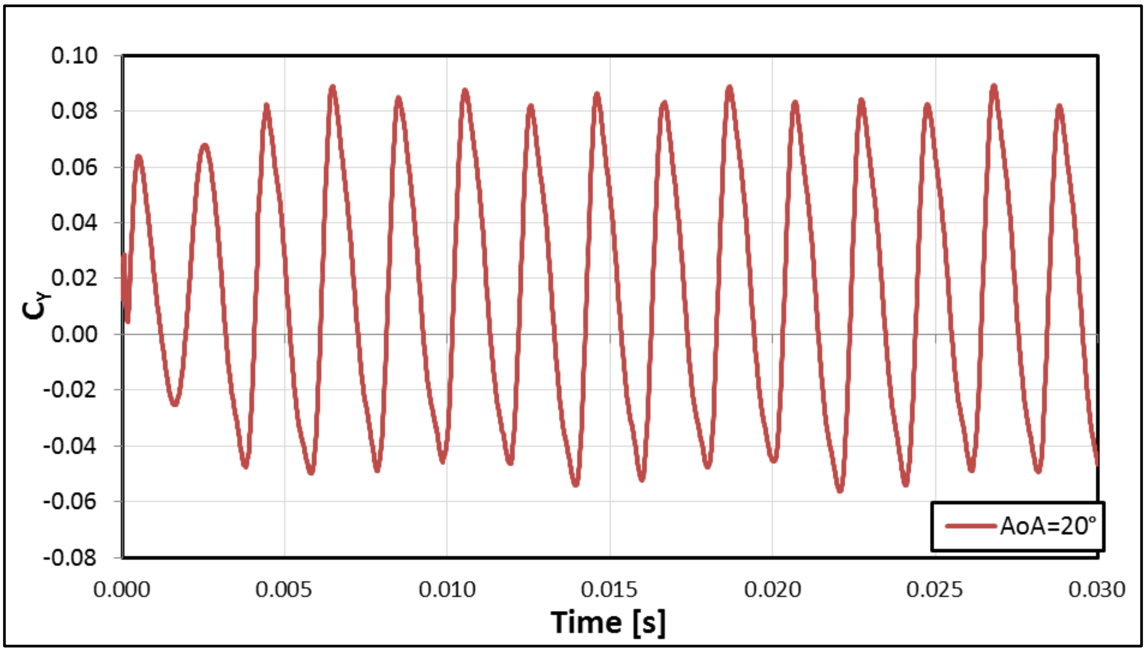

Figure 3: Change of Side Force Coefficient with respect to Time

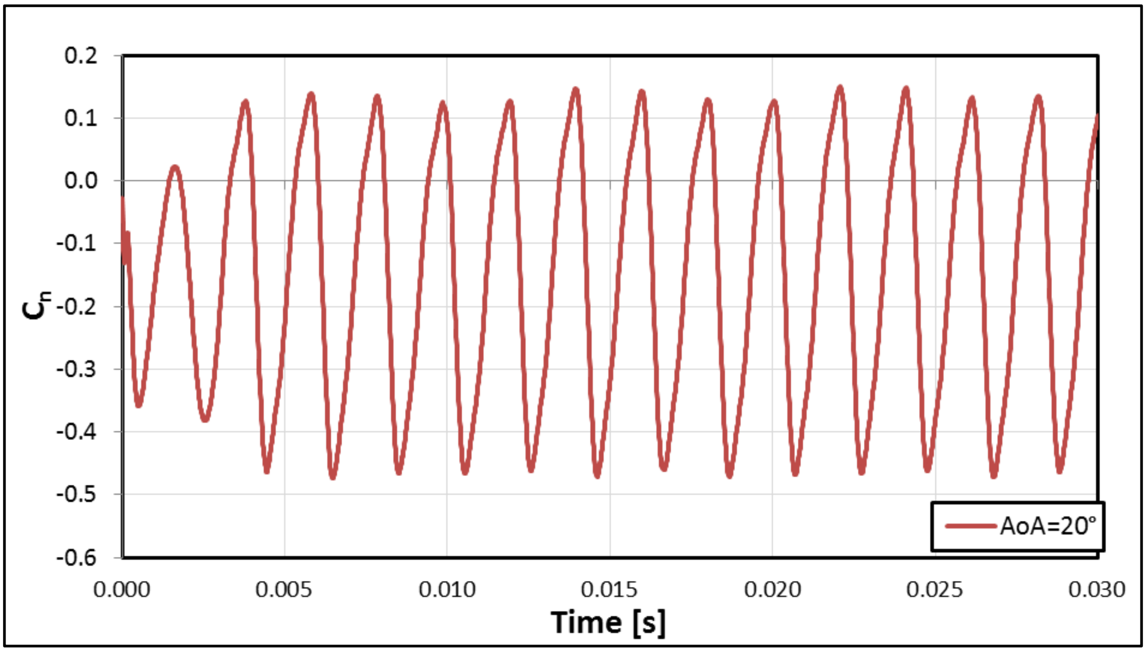

Figure 4: Change of Yaw Moment Coefficient with respect to Time

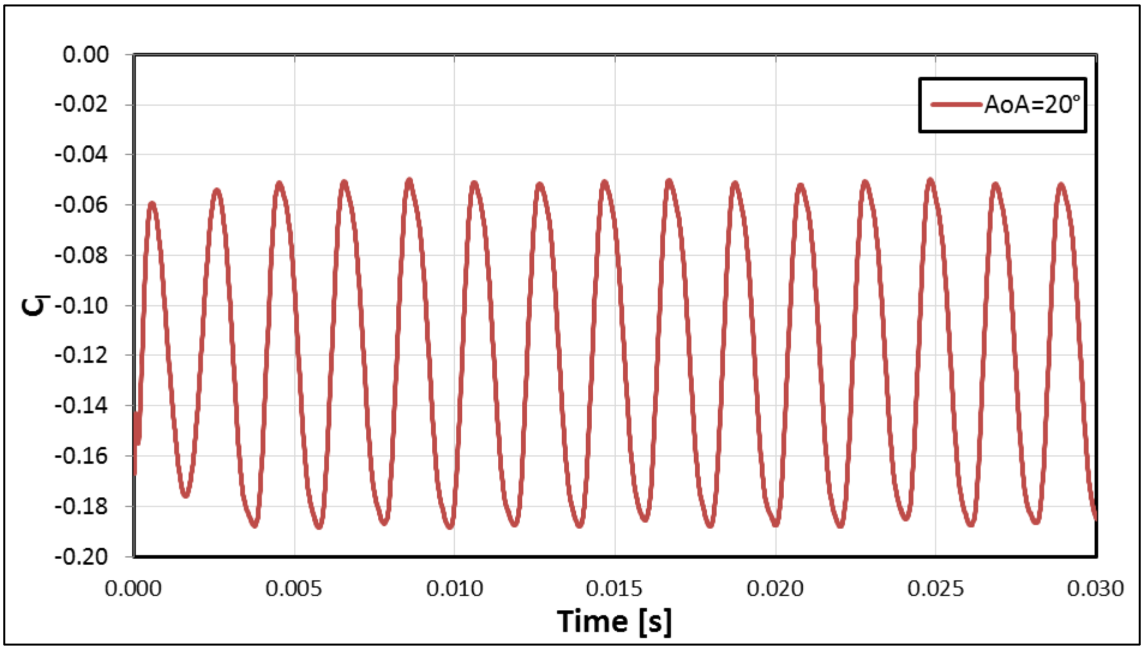

Figure 5: Change of Roll Moment Coefficient with respect to Time

From the figures, it can be seen that coefficient values become periodic after about 0.005 seconds. Averaging these periodic time-dependent values, a single value for each of the side force, yawing moment and rolling moment coefficients determined.

It is known that, for zero spin velocity, there is zero side force, yawing moment and roll moment on MBF. In addition to that, C_{Y_p}, C_{n_p} and C_{l_p} coefficients change almost linearly with non-dimensional spin rate [Bhagwandin, 2012]. Using this information and CFD results obtained at Ω=0.03, C_{Y_p}, C_{n_p} and C_{l_p} coefficients are calculated for each angle of attack.

Calculated C_{Y_p}, C_{n_p} and C_{l_p} coefficients are compared with the experiment in Figure 6-8.

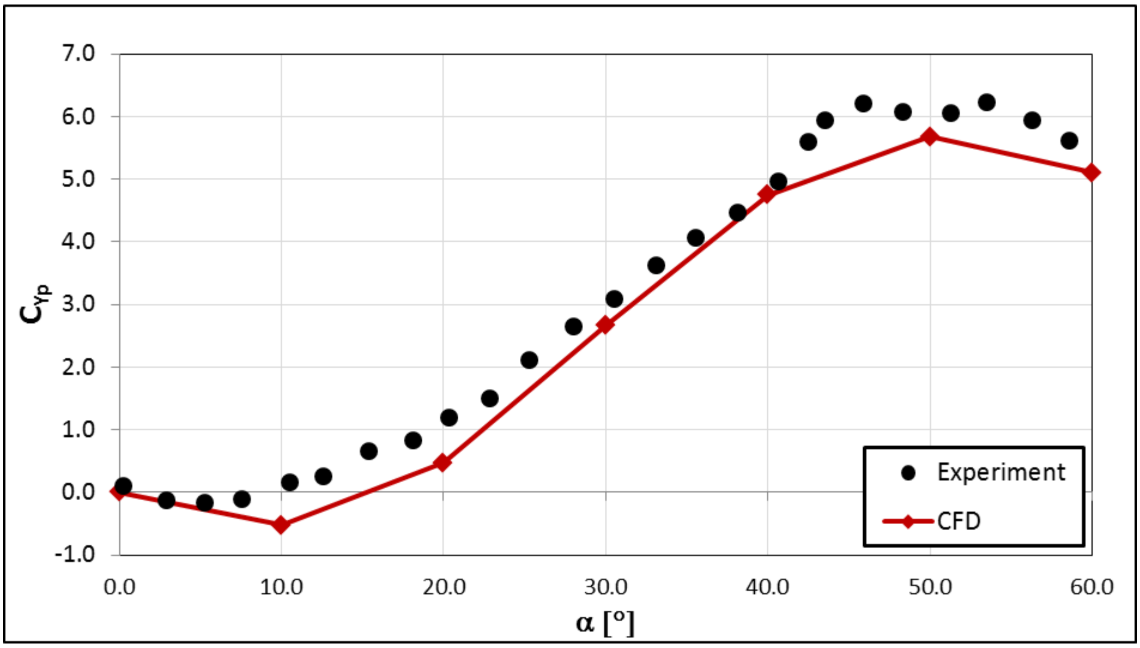

Figure 6: Change of Magnus Force Coefficient with respect to Angle of Attack

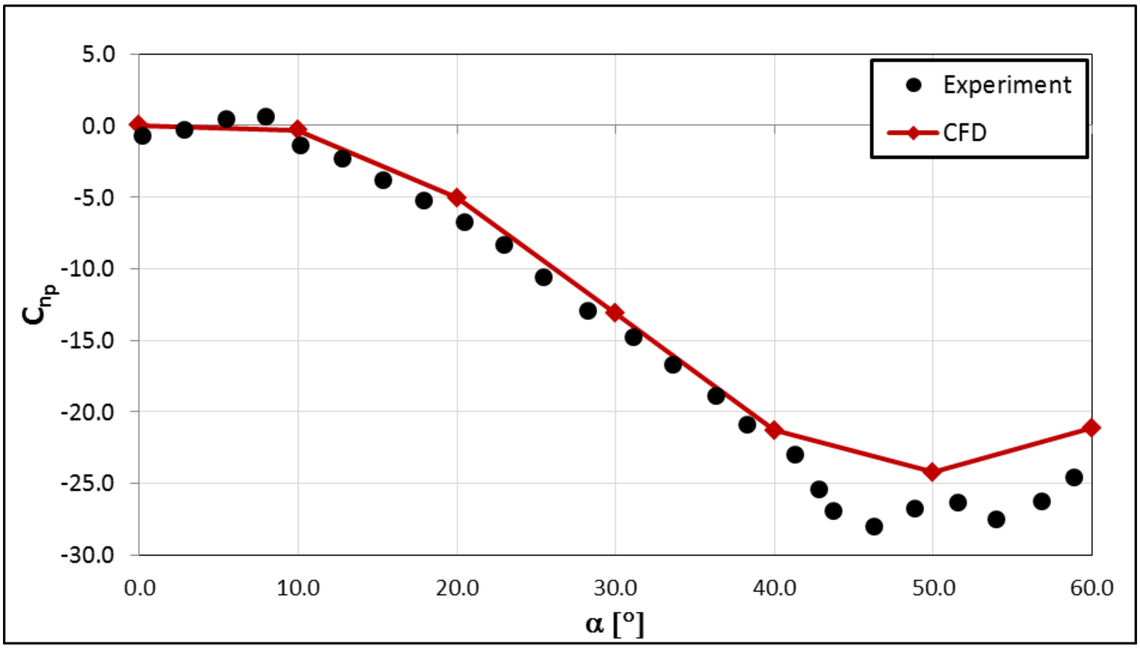

Figure 7: Change of Magnus Moment Coefficient with respect to Angle of Attack

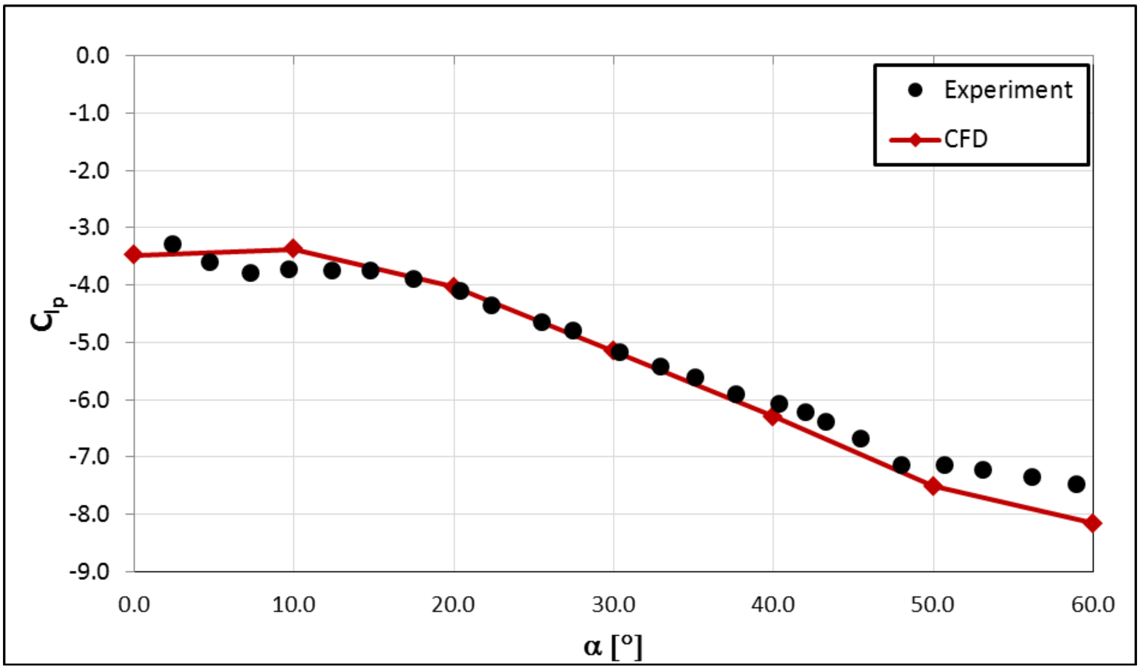

Figure 8: Change of Roll Damping Moment Coefficient with respect to Angle of Attack

Figures 6-8 show that CFD results obtained at 30° and 40° have a good agreement with experiment. Apart from these angles of attack, the Magnus force coefficient calculated by CFD has some difference with the experiment. For Magnus moment and roll damping moment, CFD results are in general more compatible with wind tunnel test results. Accordingly, CFD method used in verification accepted as adequate for investigation of fin geometry effectiveness on Magnus coefficients. Therefore, the same methodology is used for the study mentioned in the following section.

EFFECTS OF DIFFERENT FIN GEOMETRIES ON MAGNUS FORCE AND MOMENT

As mentioned, it is known that fins have a considerable effect on Magnus characteristic of spinning missiles. In this part, the effects of different fin geometries on the Magnus force, Magnus moment and roll damping coefficients are examined. Accordingly, MBF fin geometry is modified to obtain two new configurations. When generating those alternative configurations, similar static aerodynamic properties with MBF are aimed. Using HEEDS commercial optimization software and Missile DATCOM in combination, MBF is modified with decreased span (MBF-SS) and increased span (MBF-LS) fins without changing the normal force and pitching moment characteristics (Figure 12 and 13).

Roll damping, Magnus force and Magnus moment coefficients of those configurations are calculated as explained in the verification section and results are compared with MBF.

Geometry Details of the Models

Geometries of all three configurations are shown in Figures 9, 10 and 11. In Table 2, details of the fin geometric parameters are given. As mentioned, only fin geometry of MBF is modified to obtain MBF-SS and MBF-LS configurations, so missile body geometry is the same for all 3 configurations.

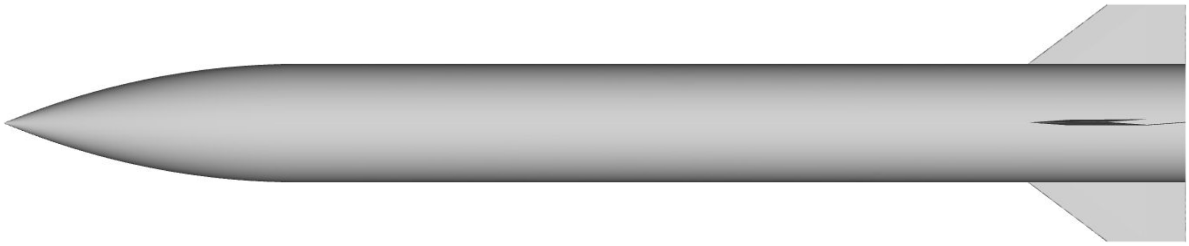

Figure 9: MBF Model

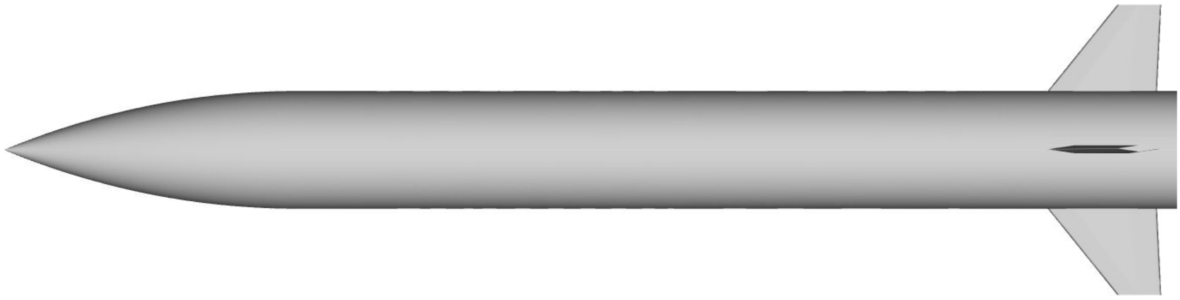

Figure 10: MBF-LS Model

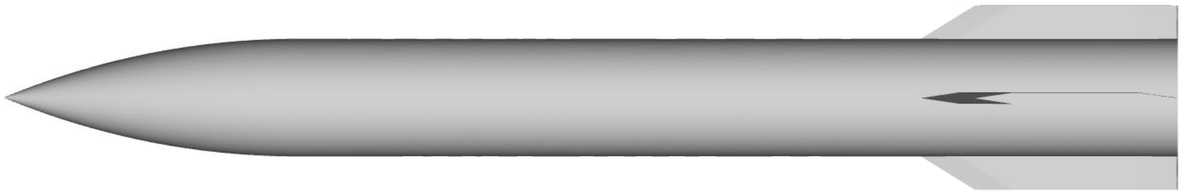

Figure 11: MBF-SS Model

Table 2: Geometry Details and Fin Locations

	MBF	MBF-LS	MBF-SS
Semi-Span [in]	0.90	1.32	0.51
Tip Chord [in]	1.20	0.67	3.11
Root Chord [in]	2.40	1.68	3.94
Aspect Ratio	0.50	1.12	0.15
Leading Edge Distance from the Missile Nose [in]	15.60	16.02	14.06

Steady Analysis Results

Before starting unsteady analyses, CFD analyses are carried out at steady-state conditions without any spin rate (Ω=0) to verify the aerodynamic performance similarity of the configurations. Normal force and pitching moment coefficients of MBF, MBF-LS and MBF-SS are given in Figure 12 and Figure 13. As seen from Figure 12, the normal force coefficient is the same for all three configurations. For pitching moment, some differences can be seen with MBF-SS having slightly higher values in all angles of attack. Nevertheless, the difference is not dramatic and it is accepted that all three configurations have similar static aerodynamic properties.

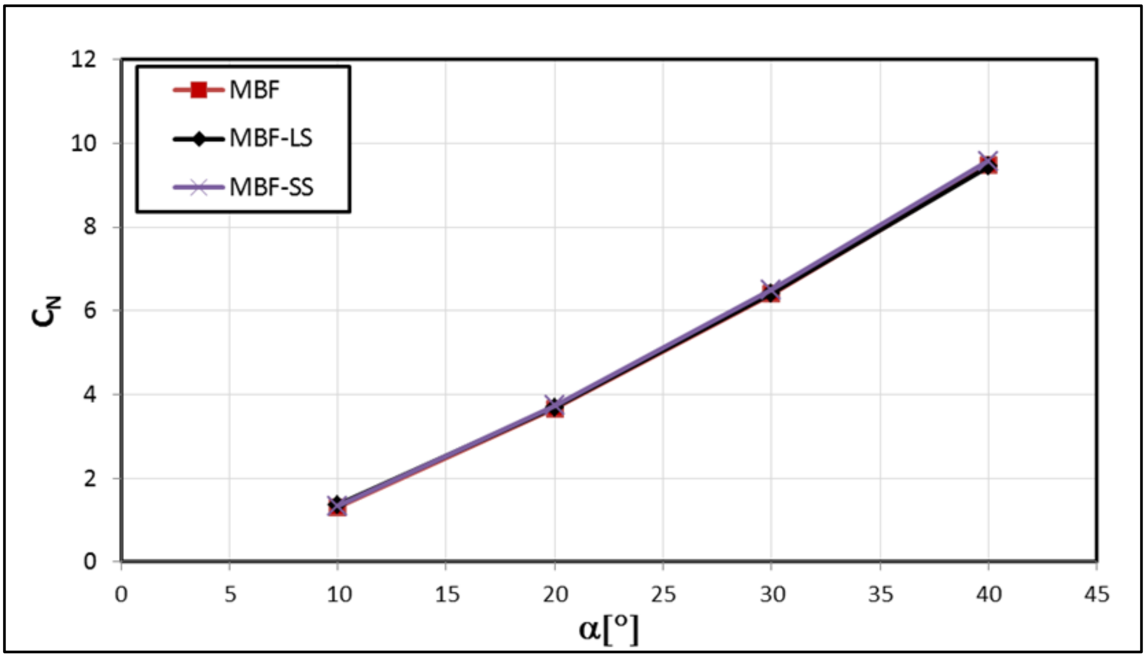

Figure 12: Change of Normal Force Coefficient with respect to Angle of Attack

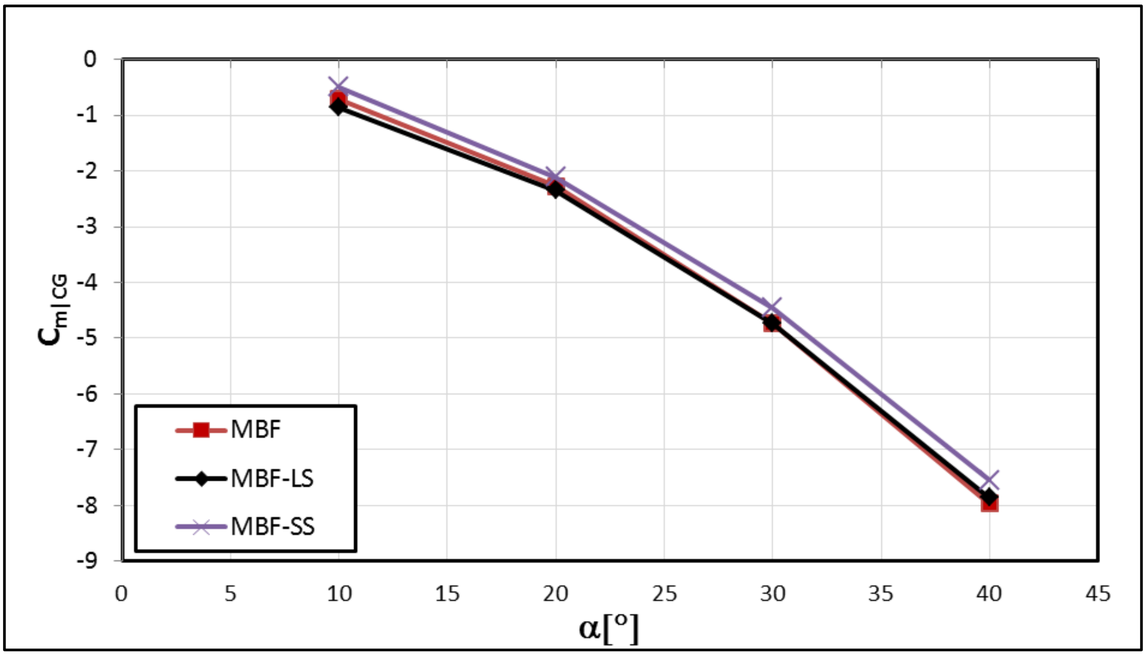

Figure 13: Change of Pitching Moment Coefficient with respect to Angle of Attack

Unsteady Analysis Results

Unsteady CFD analyses are performed to calculate Magnus force and moment at the conditions given in Table 1 for four different angles of attack (10°, 20°, 30° and 40°). As an example, the behaviors of side force coefficient, yaw moment and roll moment coefficients with changing time at 20° angle of attack are shown in Figures 13-15.

The geometry of the fins affects the aerodynamic characteristic of the missiles rotating at a high spin rate. In this study, it is found that decreasing span length and aspect ratio causes higher amplitude for side force and yaw moment coefficients; on the other hand, roll moment coefficient amplitude is decreasing. This phenomenon is valid up to 30° angle of attack.

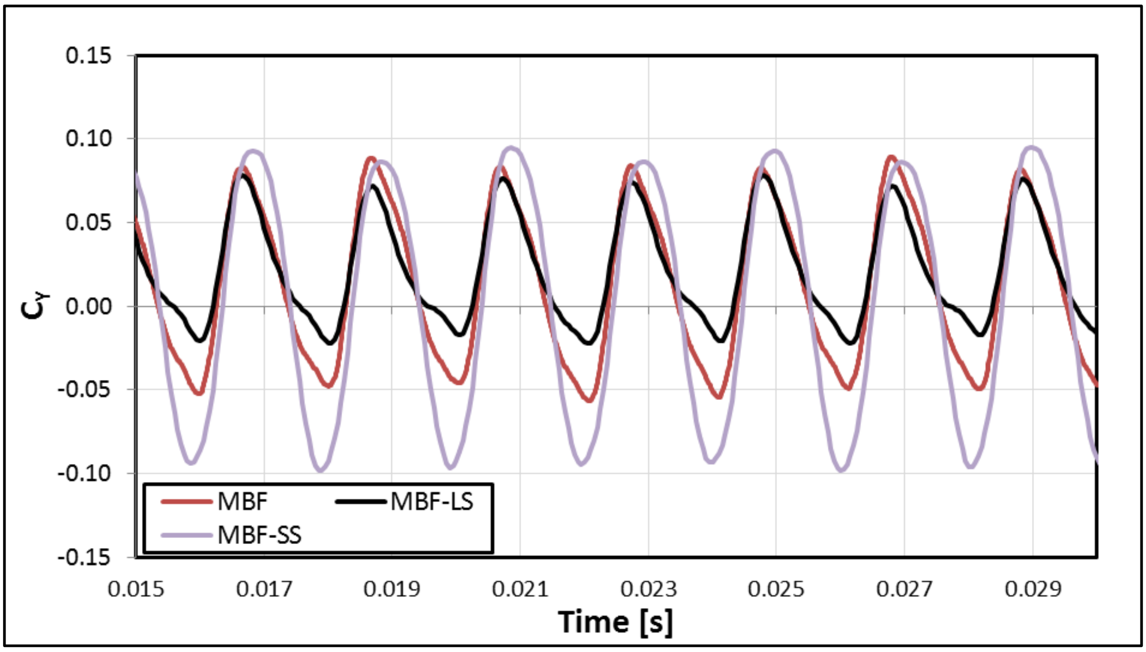

Figure 14: Change of Side Force Coefficient with respect to Time (α=20°)

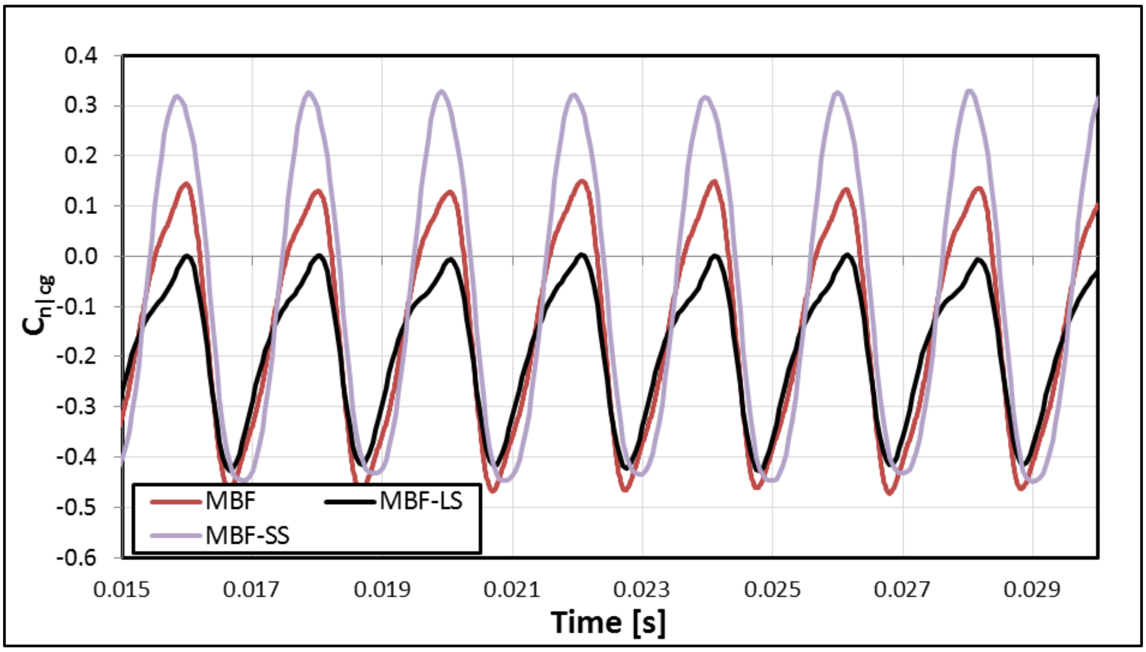

Figure 15: Change of Yaw Moment Coefficient with respect to Time (α=20°)

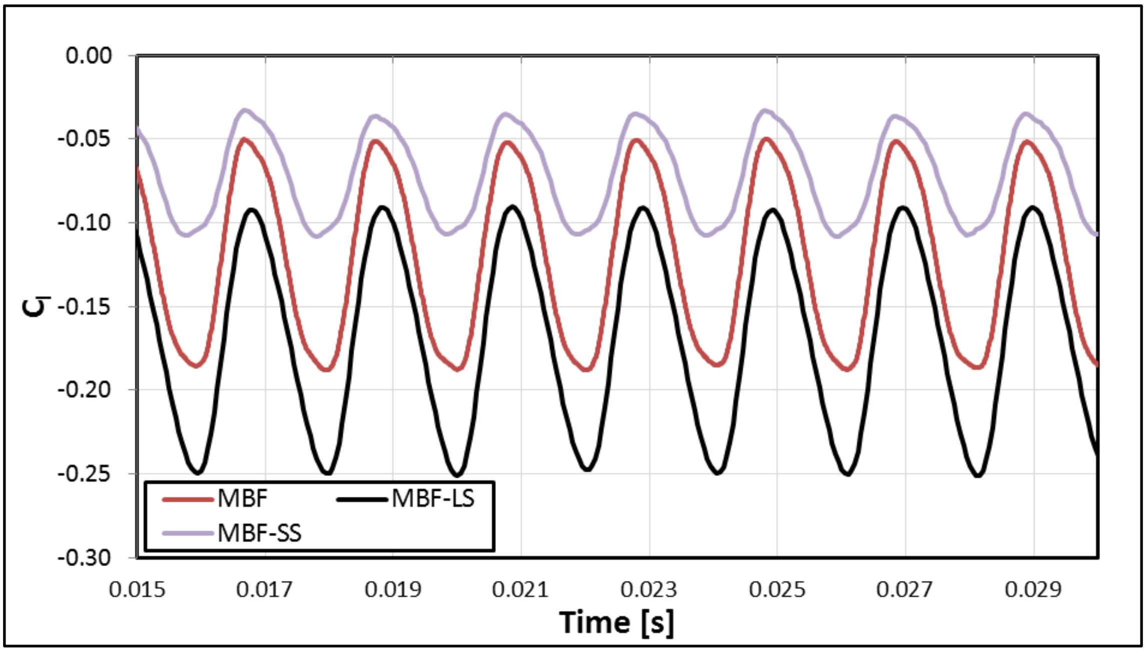

Figure 16: Change of Roll Moment Coefficient with respect to Time (α=20°)

Change of Magnus force and moment coefficients with respect to the angle of attack is given in Figure 17 and Figure 18, respectively. Results for MBF and MBF-LS are similar to each other. On the other hand, MBF-SS has less Magnus force and moment coefficient compared to the other two configurations.

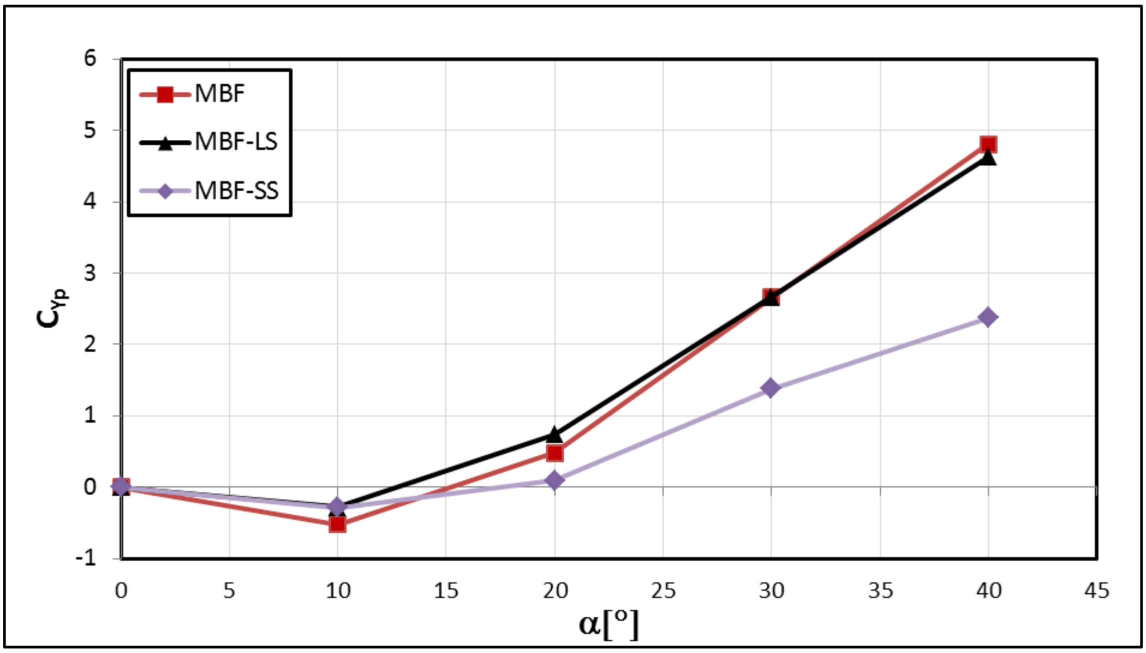

Figure 17: Change of Magnus Force Coefficient with respect to Angle of Attack

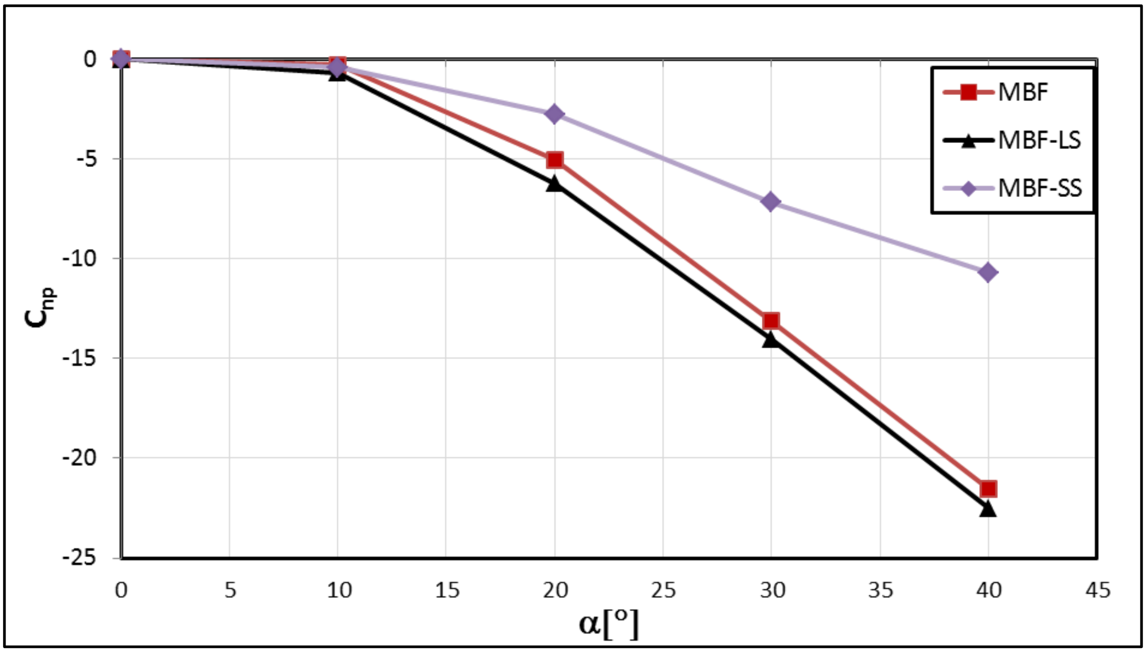

Figure 18: Change of Magnus Moment Coefficient with respect to Angle of Attack

In Figure 19, the change of the roll damping coefficient with respect to the angle of attack is presented. The magnitude of roll damping coefficient raises with increasing angle of attack for all configurations. The dependency of roll damping coefficient to the angle of attack is less for MBF-SS and more for MBF-LS configuration. It can be concluded that increasing aspect ratio of fins causes a higher magnitude of roll damping coefficient, as expected.

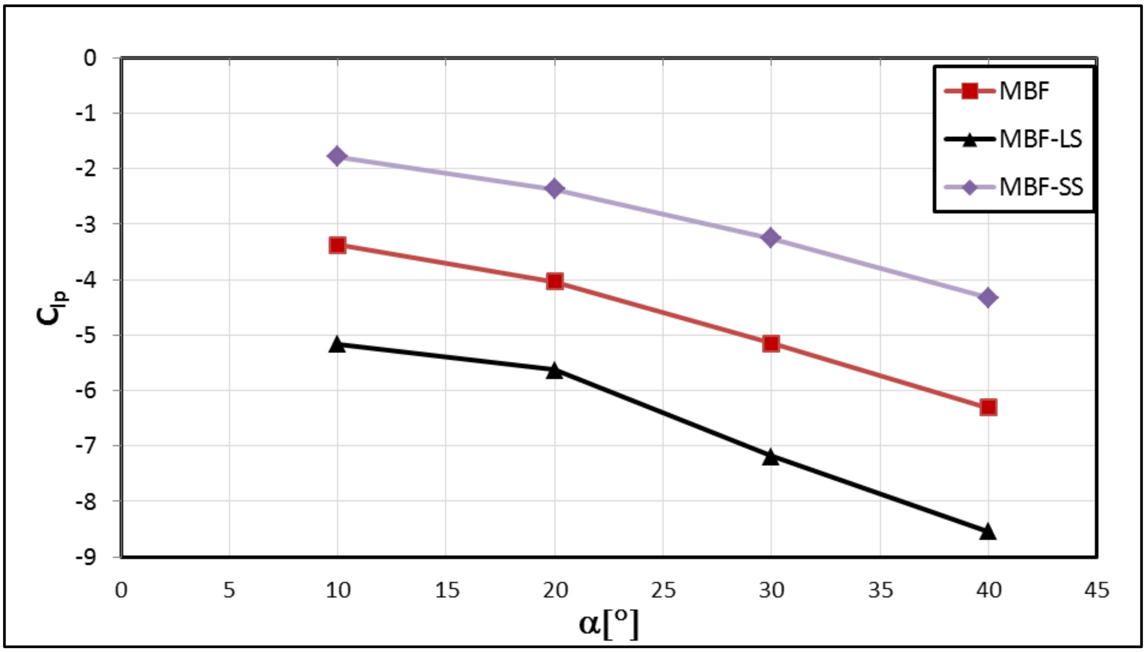

Figure 19: Change of Roll Damping Coefficient with respect to Angle of Attack

Magnus force coefficient is greater for higher aspect ratios up to 0.5 for the angle of attack above 10° as shown in Figure 20. For greater aspect ratio values than 0.5, increasing aspect ratio of fins is not affecting Magnus force value much. In Figure 21, Magnus moment coefficient is decreasing with increasing aspect ratios up to 0.5 for the angle of attack above

10°. For greater aspect ratio values than 0.5, increasing aspect ratio of fins is slightly decreasing Magnus moment value.

In contrast to Magnus coefficients, a decrease of the roll damping coefficient with increasing aspect ratio at all angle of attack range can be seen in Figure 22.

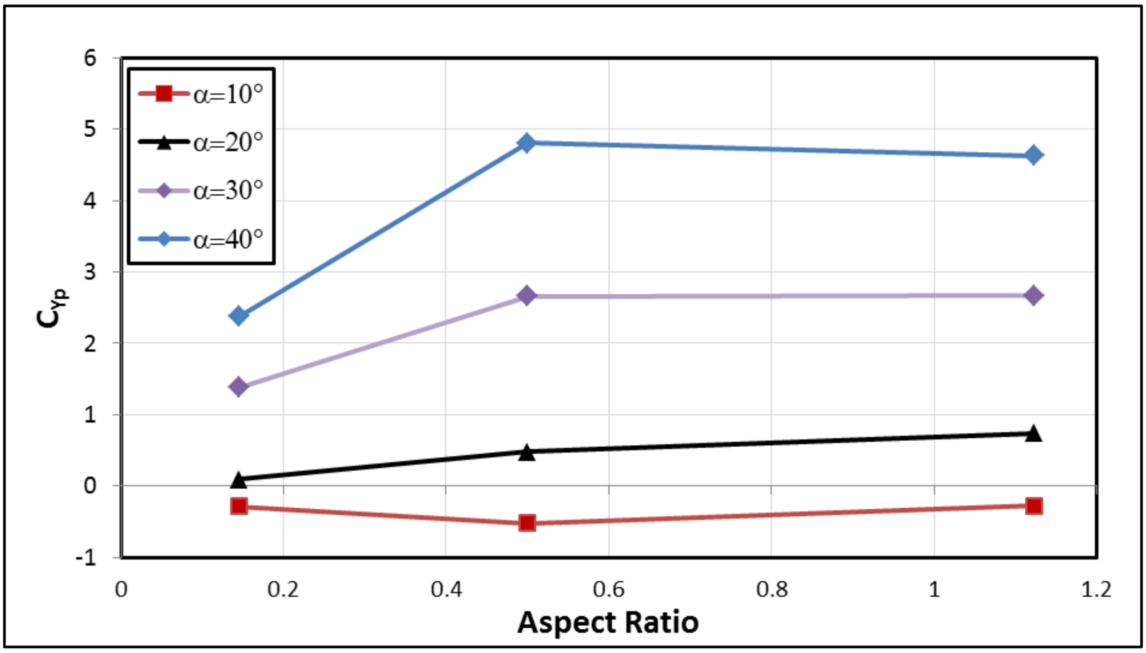

Figure 20: Change of Magnus Force Coefficient with respect to Aspect Ratio

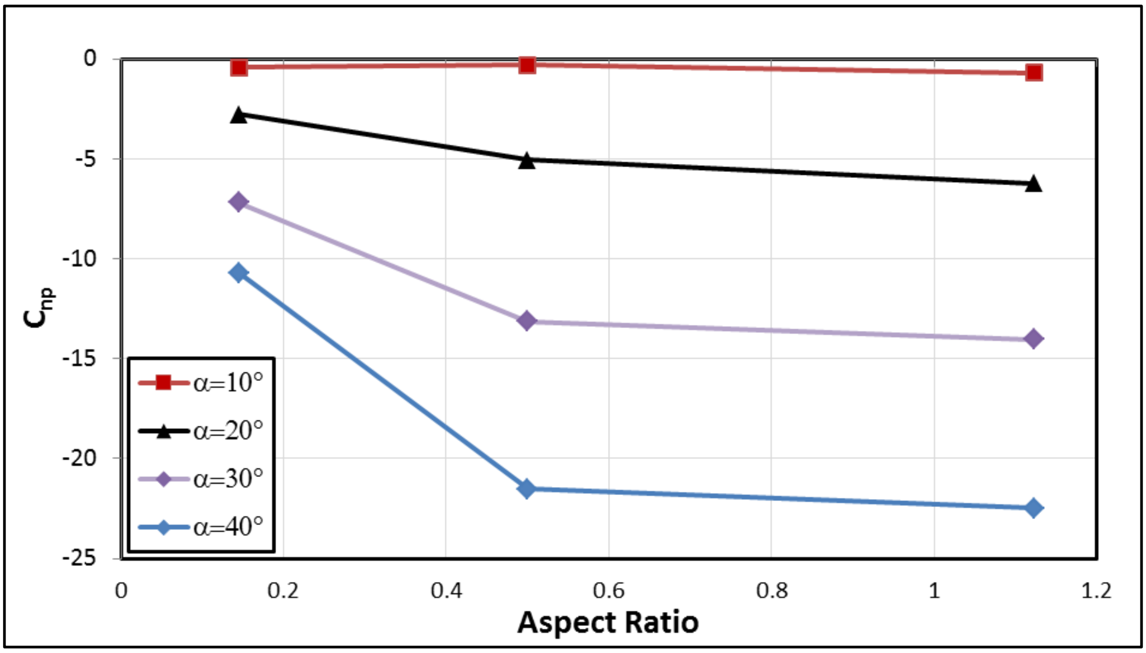

Figure 21: Change of Magnus Moment Coefficient with respect to Aspect Ratio

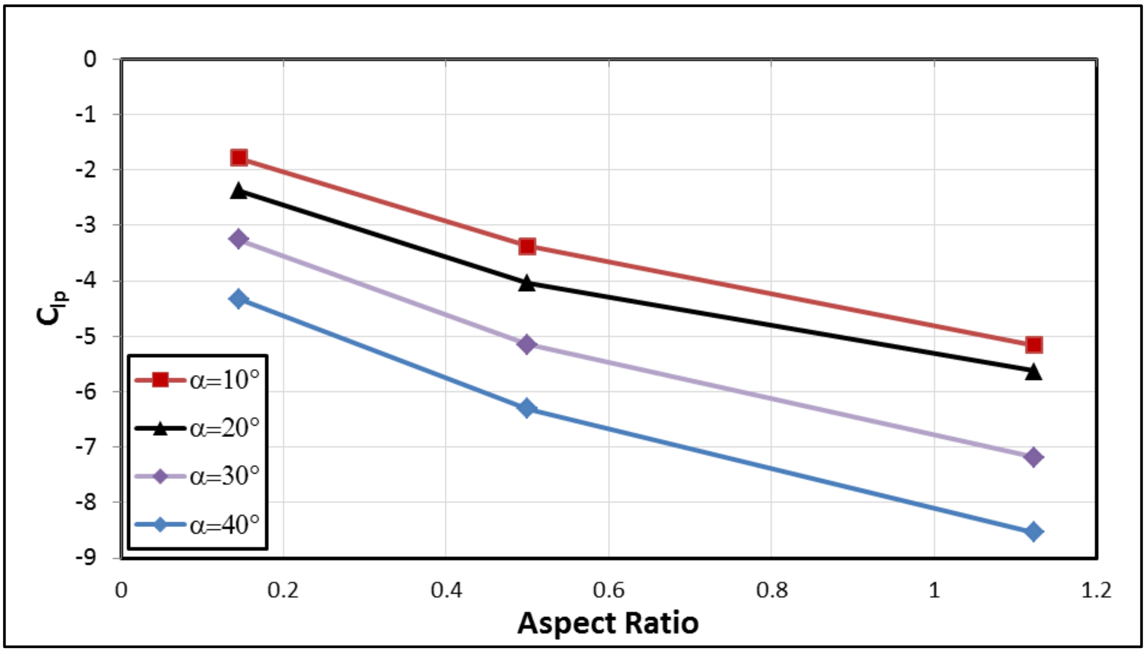

Figure 22: Change of Roll Damping Coefficient with respect to Aspect Ratio

In order to understand the effect of fin geometry on Magnus force, contributions of body and fins to the side force coefficient are investigated. Figure 23 shows the average side force coefficient generated by each component for one revolution (α=40°). All three configurations have same body geometry; however, side force generated by bodies is different. The region of body around the fins is affected by fins, resulting in difference on body side force. In addition to that, there is no general trend in the behavior of body side force with respect to aspect ratio of the fins. Nevertheless, contribution of fins to the side force increases with increasing aspect ratio. In the end, MBF and MBF-LS have similar total side force coefficients as deficiency in body force is compensated by fins for MBF-LS. Body and fin side forces are lower than the other two configurations for MBF-SS, leading to a lower total coefficient value.

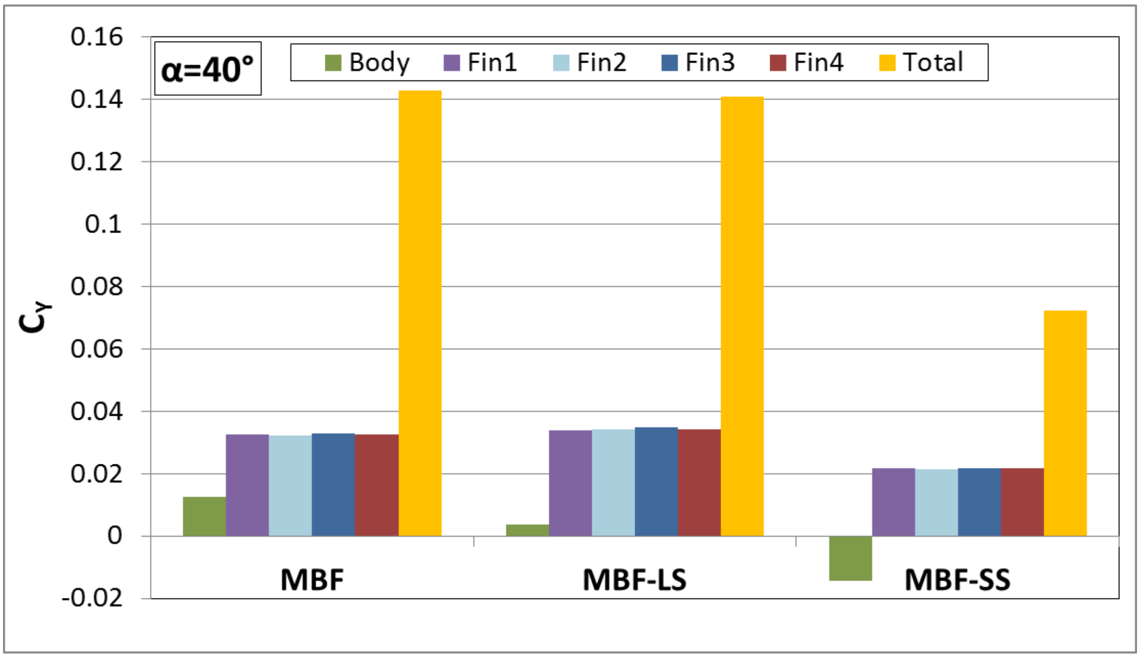

Figure 23: Side Force Contribution of Missile Components for One Revolution (Averaged)

Static pressure contours of the flow field around tail fins at α=40° are given in Figure 24-26. For Figure 24 and Figure 25, pressure contours are drawn when the roll orientation of the missile corresponds to ϕ=80.9°. On the other hand, in Figure 26 and Figure 27, roll attitude of the missile is ϕ=108.4°. Dashed lines drawn on the side views show where contour sections are created. In Figure 24 and Figure 26, pressure contours are generated at the middle of the mean chord of the fins. Pressure contours shown in Figure 25 and Figure 27 are created at tip chord leading edge location of the fins.

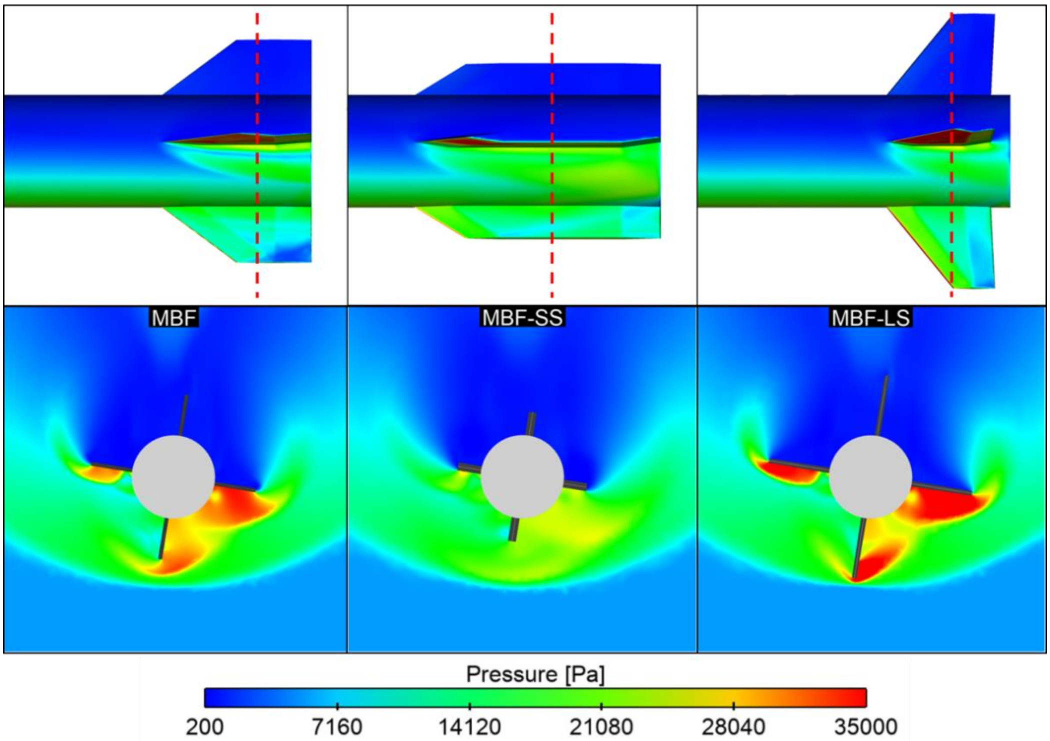

Figure 24: Static Pressure Contours around Mean Chord Midpoint of Tail Fins (ϕ=80.9°)

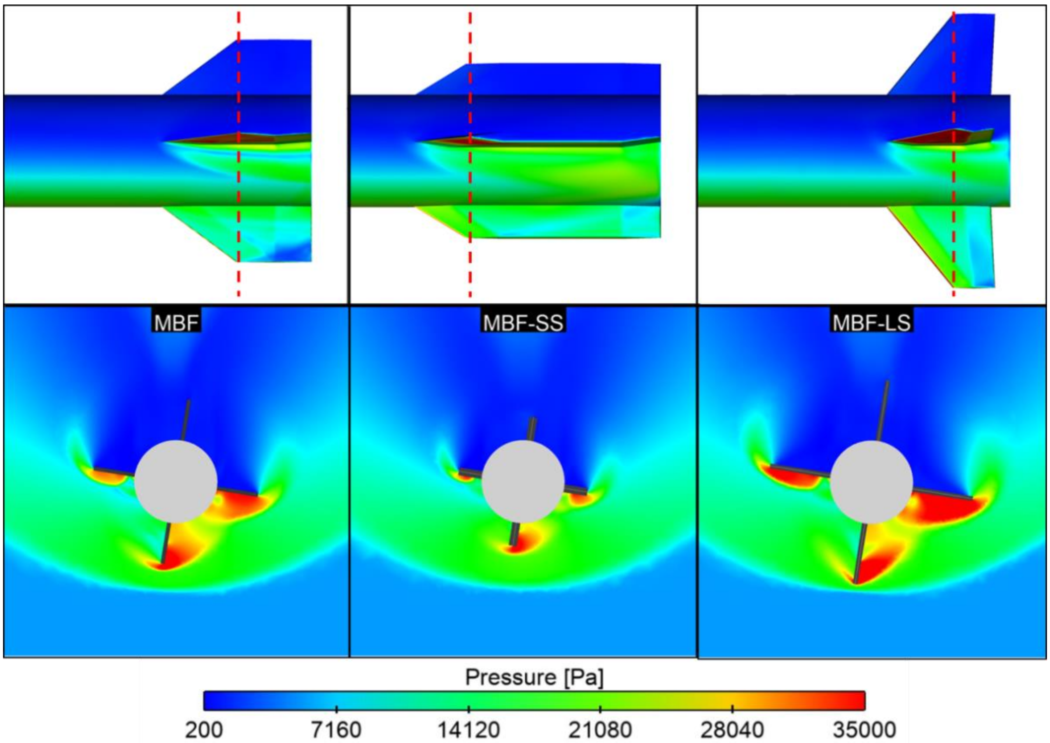

Figure 25: Static Pressure Contours around Tip Chord Leading Edge of Tail Fins (ϕ=80.9°)

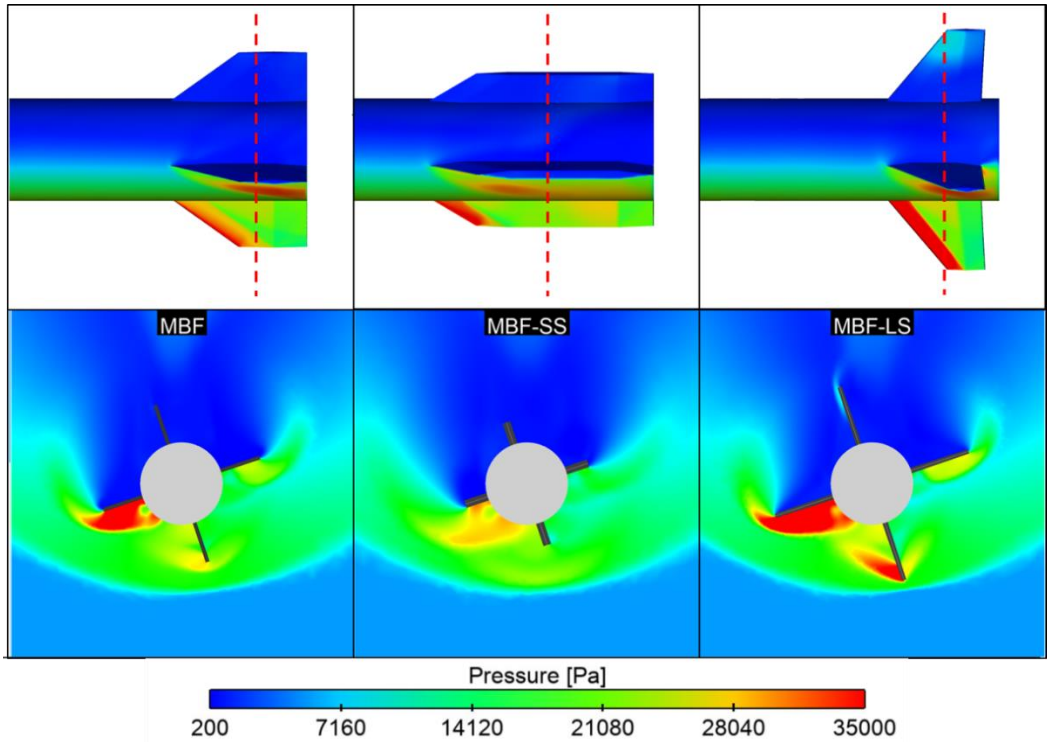

Figure 26: Static Pressure Contours around Mean Chord Midpoint of Tail Fins (ϕ=108.4°)

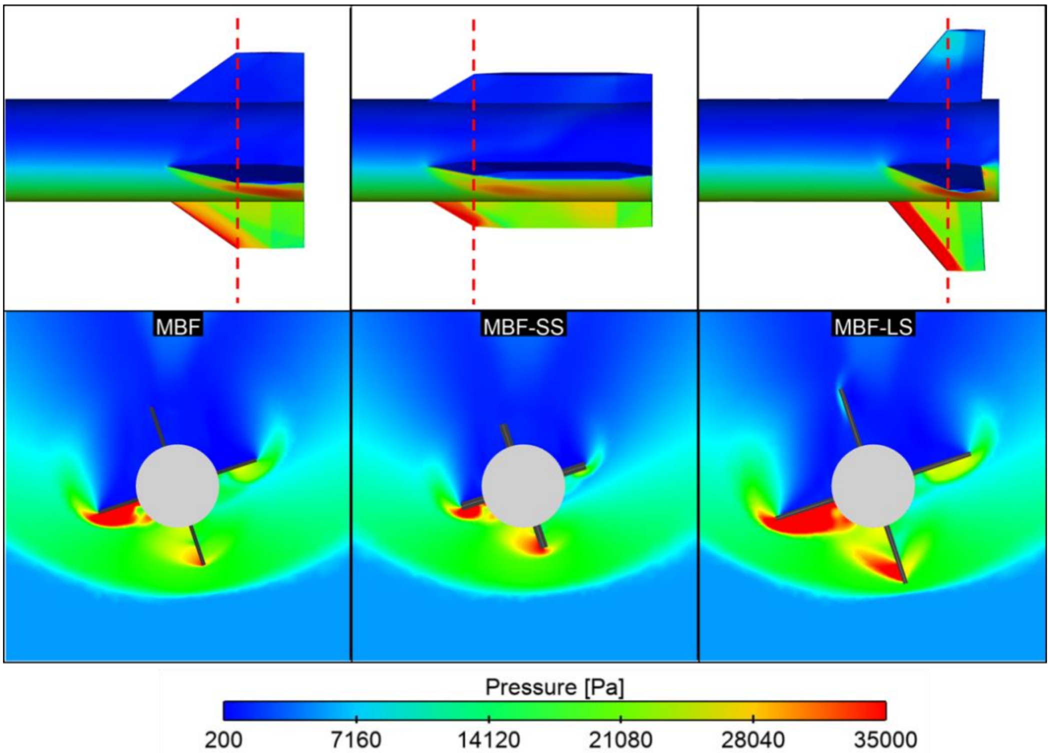

Figure 27: Static Pressure Contours around Tip Chord Leading Edge of Tail Fins (ϕ=108.4°)

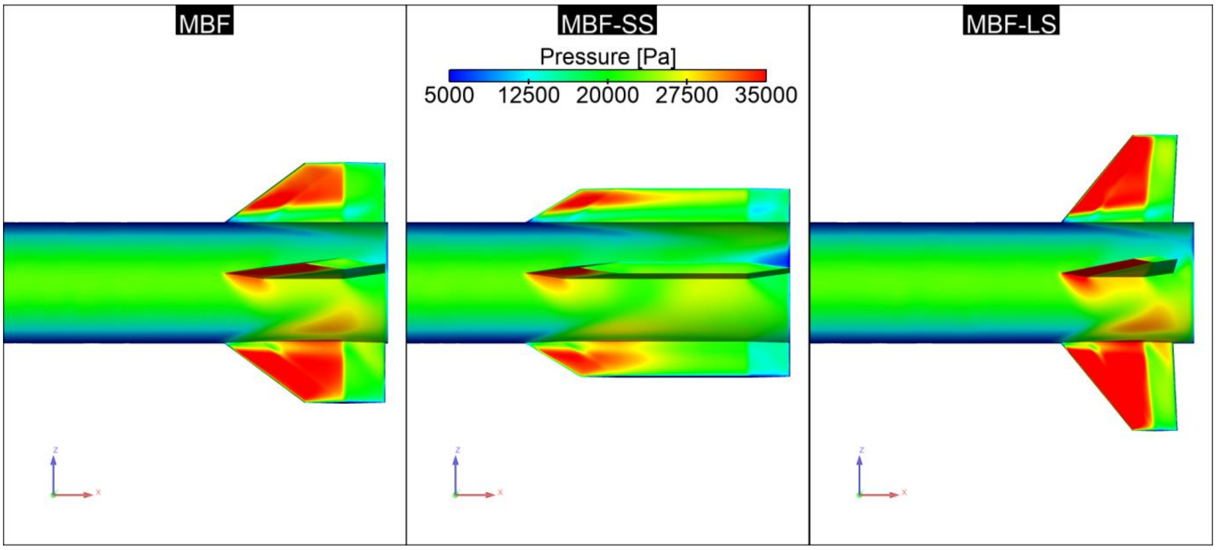

Figure 28: Static Pressure Contours on the Missiles, Bottom View (ϕ=80.9°)

In Figure 24-Figure 27, it can be seen that flowfield static pressure distributions for MBF and MBF-LS show similarities to each other. On the other hand, MBF-SS has less pressure strength and different pressure distribution around the fins. In addition to that, effect of fins on body pressure is less severe for MBF-SS as seen in Figure 28. Body force on MBF and MBF-LS fluctuates to higher magnitude values when a full rotation is considered. These explain Magnus force and moment similarities of MBF and MBF-LS; different Magnus force and moment characteristics of MBF-SS. Moreover, in Figure 26 and Figure 27, some part of the upper tail of MBF-LS has higher pressure than the other configurations'. The larger span of MBF-LS enables its upper fin to get rid of wake region of the body. This difference contributes to higher fin side force and roll damping value of MBF-LS compared to the other configurations.

CONCLUSIONS

In this study, steady and unsteady CFD analyses of Modified Basic Finner (MBF) test case and two additional configurations with modified MBF fin sets are performed. It is aimed to examine the effects of fin geometry on Magnus and roll damping characteristic of the missiles. CFD analyses are carried out for 2.5 Mach number at wind tunnel test conditions. In the first part of the study, MBF is rotated at 773.3 rad/s by performing unsteady CFD analyses. Then, Magnus force, Magnus moment and roll damping coefficients are calculated and compared with wind tunnel test results for method verification. Consistency between CFD and wind tunnel test results is seen. In the second part of the study, two different configurations are generated by considering a similar pitch plane aerodynamics with MBF. Unsteady CFD analyses of these two configurations are performed and results are compared with MBF. Results show that Magnus characteristic of MBF and MBF-LS is similar to each other, whereas MBF-SS has less magnitude of Magnus force and moments compared to others. Difference on body pressure distribution around the fins has important effect on Magnus. On the other hand, roll damping is directly affected by the aspect ratio. Increasing aspect ratio causes a higher roll damping magnitude. Pressure contours show that configuration with low aspect ratio fins (MBF-SS) has different pressure distribution around the fins compared to the other two configurations.

To sum up, very low aspect ratio fins can be used to have low Magnus effects on spinning missiles. Increasing the aspect ratio value affects Magnus characteristics up to some point. However, for roll damping coefficient, aspect ratio almost linearly affects the coefficient value.

References

Bhagwandin V. A. (2012) *Numerical Prediction of Roll Damping and Magnus Dynamic Derivatives for Finned Projectiles at Angle of Attack,* 30th AIAA Applied Aerodynamics Conference 25 - 28 June 2012

Bhagwandin V. A. (2016) *High-Alpha Prediction of Roll Damping and Magnus Stability Coefficients for Finned Projectiles*, Journal of Spacecraft and Rockets, Vol 53, No.4, July-August 2016

Jenke L. M. (1976) *Experimental Roll-Damping, Magnus, and Static-stability Characteristics of Two Slender Missile Configurations at High Angles of Attack (0 to 90 deg) and Mach Numbers 0.2 through 2,5*, Arnold Engineering Development Center, July 1976

Pechier M., Guillen P.(2001) *Magnus Effect over Finned Projectiles ,*Journal of Spacecraft and Rockets, Vol. 38, No:4, July - August 2001

Samardzic M., Anastasijevic Z., Marinkoviski D.(2007) *Some Experimental Results of Subsonic Derivative Obtained in the T-38 Wind Tunnel by Forced Oscillation ,*Scientific Technical Review, Vol. LVII, NO. 3-4, 2007